STRONG OXIDANTS FOR ORGANIC WASTE DESTRUCTION FROM OXIDATION OF MANGANESE HYDROXIDE

D.K. Cha[*] and S.-M. Park, Department of Chemistry, University of New Mexico, Albuquerque, NM, 87131

ABSTRACT The redox chemistry of $Mn(OH)_2$ has been studied at manganese electrodes in 0.10 *M* KOH solutions employing transient electrochemical techniques in an effort to elucidate mechanisms involved. The charge transfer process is shown to be affected by the film formed on the electrode surface during redox processes. The Mn(0)/Mn(II) and Mn(II)/Mn(III) pairs, which have not been reported hitherto clearly in the literature, has been observed using techniques such as chronopotentiometry and differential pulse voltammetry. Electrode potentials for these redox processes, i.e., between $Mn(OH)_2$ and higher valence oxides as well as the manganese metal, have been assigned. Diffusion coefficients of reactant molecules through the $Mn(OH)_2$ film and exchange rate constants for redox processes are also reported.

KEYWORDS: manganese oxidation, redox potential, diffusion coefficient

INTRODUCTION

The electrochemical oxidation of manganese is an important subject since its oxidation produces different products with oxidation states of +2 through +7 depending on experimental conditions. Mn(IV) is useful mainly as electrolytic manganese dioxide (EMD), which is an important cathode material for high performance batteries. As a result, the electrochemical reduction of manganese dioxide has received much attention. Due to its importance, numerous papers have been published [1-11]. The subject has also been reviewed [12].

Many studies have been conducted to identify the intermediate species formed during the oxidation of Mn(II) to MnO_2. Fleischmann, *et al.* [5] postulated several adsorbed Mn(III) and Mn(IV) species to interpret the electrochemical behavior. Paul and Cartwright [6, 7] proposed a mechanism involving the oxidation of manganous ions at the growing MnO_2 deposit to produce a relatively stable solid intermediate species. Gosztola and Weaver [8] concluded that MnOOH plays certain roles in the oxidation process. Kao and Weibel [9] reported that the oxidation of Mn(II) to Mn(III) is followed by a disproportionation reaction to produce Mn(II) and MnO_2, initiating the deposition of EMD. Conway, *et al.* [10, 11] reported the detection of Mn(III) on chemically-modified MnO_2 cathodes in strong alkaline solutions. Randle and Kuhn studied the oxidation of Mn(II) to Mn(III) at platinum [13] and PbO_2 [14] electrodes. They demonstrated that the reaction order is one for both the oxidation of Mn(II) to Mn(III) and the reduction of Mn(III) to Mn(II). We have also reported the oxidation of Mn(II) in perchloric acid solutions [15].

Anodic oxidation of manganese in alkaline media has received attention due to its technological relevance, and the process has been investigated extensively in an effort to

[*] To whom all correspondence should be addressed (e-mail: dkcha@unm.edu).

understand corrosion/passivation phenomena of manganese electrodes [16-26]. The oxidation of manganese in alkaline media may be described as consisting of two or more steps: to manganese(II) hydroxides at a lower applied potential and to higher oxidized states at more positive potentials. $Mn(OH)_2$ thus produced on the electrode surface may be oxidized further to MnOOH. The presence of intermediate species such as $[Mn(OH)_4]^{2-}$ and $[Mn(OH)_3]^-$ has been suggested by Kozawa and Yeager [1, 3]. However, direct evidence for these species has not been observed in voltammograms.

Use of the manganese electrode would be advantageous for studying the overall electrochemical reactions of manganese and its hydroxides/oxides rather than use of an inert electrode such as platinum. We thus employed a manganese electrode to examine the redox chemistry involved in 0.10 *M* KOH. It is also interesting to determine the $Mn(OH)_2$/Mn redox potential, as its published value [27] might represent the one calculated from the thermodynamic data. As in the case of the Mn^{2+}/Mn(0) system in nearly neutral media [19], the system shows an electrochemical and chemical reversibility in alkaline media.

As part of our efforts to investigate the oxidation of metals [15, 28-34] and their possible applications to indirect oxidation of organic compounds [35], we report here our results on manganese oxidation. The diffusion coefficients of hydroxide ions during the oxidation of $Mn(OH)_2$ to MnOOH and to passive films have been determined, and a diffusion model for the electron transfer reaction is discussed.

PROCEDURES

A manganese metal piece with a flat surface (Johnson Matthey, 99.99%) was used as a working electrode. It was sealed to Pyrex glass tubing with wax, and its exposed geometric area is about 0.75 cm^2. A Ag/AgCl (in saturated KCl) electrode and a platinum foil were used as reference and counter electrodes, respectively. Reagent grade KOH (J.T. Baker) was used as received to make up 0.10 *M* KOH solutions with doubly distilled water. All these electrodes were housed in a single compartment cell.

The working electrode was polished to a mirror finish with various grades of emery papers and rinsed thoroughly with doubly distilled water. All the experiments were carried out at room temperature under an argon atmosphere after the solution had been thoroughly purged with argon. A fresh working electrode covered with $Mn(OH)_2$ was prepared by stepping the potential to -1.50 V vs. Ag/AgCl for 20 minutes prior to each experiment. Attempts to produce a pure metal surface by electrochemical reduction were not successful due to high reactivity of Mn. Any oxide films of higher valences, therefore, must have been reduced to manganese(II). The Pourbaix diagram predicts a stable region for $Mn(OH)_2$ at this potential [36].

Electrochemical measurements were made with a Princeton Applied Research (PAR) model 273 potentiostat/galvanostat. Unless otherwise mentioned, all the potentials were measured and quoted with respect to the Ag/AgCl (in saturated KCl) electrode.

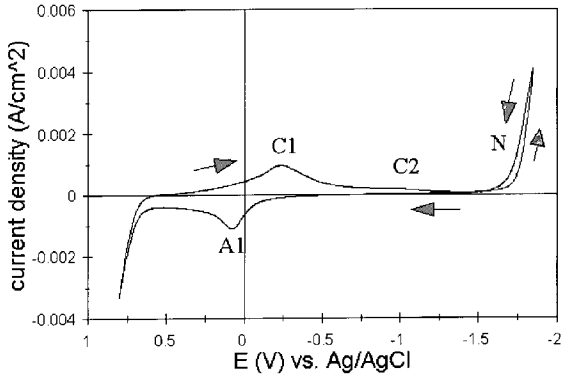

FIGURE 1. CYCLIC VOLTAMMOGRAM OF MANGANESE ELECTRODE IN 0.10 *M* KOH. THE SCAN RATE WAS 50 mV/s.

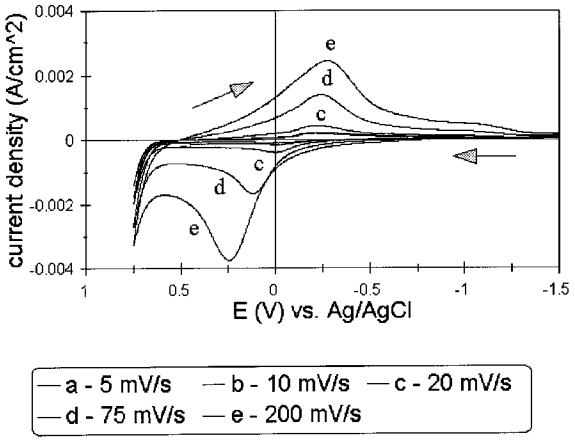

FIGURE 2. CYCLIC VOLTAMMOGRAMS OF MANGANESE ELECTRODE IN 0.10 *M* KOH. SCAN RATES IN INCREASING CURRENTS WERE: (a) 5, (b) 10, (c) 20, (d) 75, (e) 200 mV/s. THE REMAINING SCAN RATES SUCH AS 50, 100, 500, AND 1,000 mV/s WERE OMITTED FOR CLARITY.

RESULTS AND DISCUSSION

Cyclic voltammetry

A cyclic voltammogram (CV) recorded during the first cycle is shown in Figure 1, which is in good agreement with those published in the literature [18, 37]. A few observations can be made on this CV. Firstly, the CV remained the same even after a few potential sweeps as the working electrode reached a steady state rapidly. Secondly, the current peak C2 was seen only at higher scan rates as shown in Figure 2, when higher currents were observed. Thirdly, the anodic counterpart of C2 was never seen in CVs at any scan rates. Probably the amount of the species undergoing a reaction at this potential was too small to be detected on CVs, or it might indicate a short-lived intermediate species during the transition from Mn(II) to higher valence oxides.

From various experiments reported in the literature [17, 22, 23, 36] for manganese oxidation in alkaline solutions, the CV peaks shown in Figure 1 can readily be assigned. The large anodic peak marked as A1 results from passivation of the electrode surface.

The large cathodic peak marked as C1 corresponds to reduction of A1. This passivation layer seems to be MnO_2, hydroxides, and/or mixed oxides such as $MnO_x(OH)_y$ [16, 22] because the layer results from oxidation of manganese(II) hydroxide and/or manganese(III) oxyhydroxide. Peak C2 exhibits reduction of MnOOH to $Mn(OH)_2$ [23]. The anodic counterpart of C2 is not detected in cyclic voltammograms; this redox process will be discussed in more detail below. The redox reaction taking place at the A1/C1 wave may be represented as [16, 22]

$$MnO_x(OH)_y + zH_2O + ze^- = MnO_{x-z}(OH)_{y+z} + zOH^-. \quad (1)$$

Equation 1 shows a certain degree of reversibility, which allows the anodic and/or cathodic processes to be identified by electrochemical techniques.

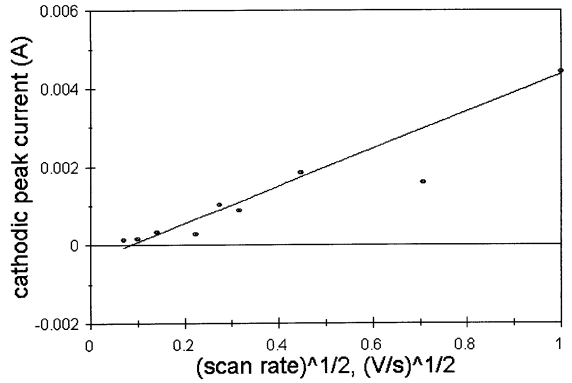

FIGURE 3. SCAN RATE DEPENDENCY OF CATHODIC PEAK CURRENTS SHOWN IN FIGURE 2.

The region N in Figure 1 corresponds to the nucleation loop for the manganese metal from reduction of $Mn(OH)_2$. The reduction of $Mn(OH)_2$ is often obscured in a voltammogram due to its proximity to hydrogen evolution.

Figure 2 shows the scan rate dependency of the voltammogram. The scan rate affects both the potential and the current density for the anodic wave. Note that peak A1 has shifted to more positive potentials at faster scan rates while the potential of the peak C1 remained relatively constant. Another cathodic peak, C2 shown in Figure 1, becomes more pronounced at faster scan rates. Also, peak separations become larger at higher scan rates as pointed out above. This indicates that a slow electron transfer is involved, particularly during the anodic scan. The large potential shift in the anodic direction could also be associated with changes in the composition of the passivation layer during the anodic scans.

Both the anodic and cathodic peak currents for CV peaks A1 and C1 show an approximate linear dependency on the square root of scan rates. Shown in Figure 3 is the scan rate dependency of the cathodic peak (C1) current, which is reasonably linear with the exception of the peak current at 500 mV/s and those at very slow scan rates. This indicates that the formation of the passive layer must be diffusion limited.

For an electrochemically-reversible system [38], the Randles-Sevcik equation [41, 42] relates the peak current, i_p, with the scan rate, υ, according to

$$i_p = (2.69 \times 10^5)\, n^{3/2} A D_o^{1/2} C_o^* \upsilon^{1/2}, \quad (2)$$

where n is the number of electrons transferred, A the electrode area in cm^2, C_o^* the bulk concentration of MnO_2 in mol/cm^3 undergoing the electrochemical reduction, and D_o the diffusion coefficient of a reactant in cm^2/s. Examination of Equation 2 reveals that the plot of i_p vs. $\upsilon^{1/2}$ allows us to obtain the diffusion coefficient. The n should be 2.0, because we mainly have the reduction of MnO_2 to $Mn(OH)_2$ according to

$$MnO_2 + 2H_2O + 2e^- = Mn(OH)_2 + 2OH^-. \quad (3)$$

The diffusion coefficient thus obtained from the scan rate dependency is 2.1×10^{-14} cm^2/s. The concentration of MnO_2 was estimated by dividing its density, $5.03\ g/cm^3$, by its molecular weight [40], assuming that the major reaction here is represented by Equation 3. The diffusion coefficient estimated here is significantly smaller than those observed in liquid phases. It suggests that the diffusion of the hydroxide ions through a solid matrix limits the process during the redox chemistry taking place between Mn(II) and higher valence states.

One more equation relates i_p with the CV peak potential [38], E_p as

$$i_p = 0.227 n F A C_R^* k^o \exp[\alpha n_a F(E_p - E^{o'})/(RT)] \quad (4)$$

where k^o is the exchange rate constant in cm/s and $E^{o'}$ is the standard electrode

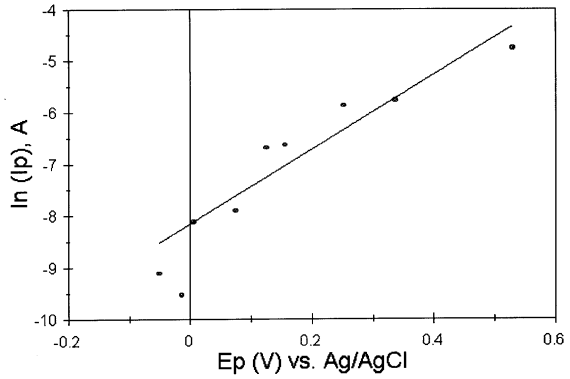

FIGURE 4. THE ln (i_p) VS. E_p PLOT EXCLUDING A PEAK POTENTIAL WHEN THE SCAN RATE WAS 5 mV/s.

potential in V. According to Equation 4, a plot of ln(i_p) vs. (E_p-$E^{o'}$) should also yield a straight line with a slope of $\alpha n_a F/(RT)$, and an intercept of ln($0.227nFAC_R^*k^o$), from which k^o values can be evaluated, provided $E^{o'}$ is known. Analyzing plots shown in Figure 4, we obtain an exchange rate constant of about 6.2 x 10^{-8} cm/s and an αn_a value of 0.19 for the anodic process. The $E^{o'}$ value [39] of -0.19 V vs. Ag/AgCl was used for this calculation. The concentration of $Mn(OH)_2$ was also estimated by dividing its density, 3.26 g/cm^3, by its molecular weight [40].

Chronopotentiometry

In an effort to identify electrochemical processes where a number of other processes take place concurrently, we used chronopotentiometry [30]. Typical chronopotentiogram (a) and the resulting dE/dt plot (b), recorded during the galvanostatic oxidation of $Mn(OH)_2$ on the manganese electrode at a current of 0.15 mA, are shown in Figure 5. The dE/dt plot shown here provides a means of determining the transition time, τ, as was used by some investigators [43, 44].

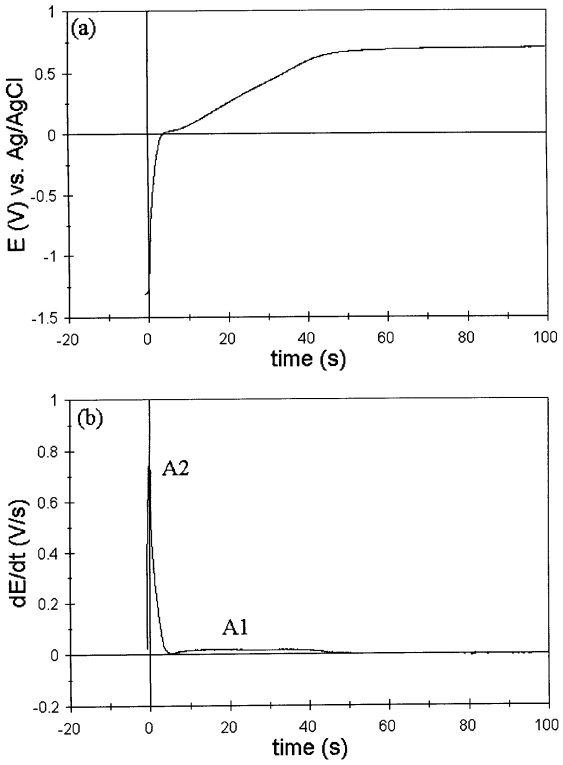

FIGURE 5. (a) CHRONOPOTENTIOGRAM RECORDED FOR ANODIC OXIDATION. THE APPLIED CURRENT WAS 0.15 mA. (b) CORRESPONDING dE/dt VS. t PLOT.

A few more reaction steps than the ones pointed out on the CV can be identified in Figure 5(b). $Mn(OH)_2$ is rapidly consumed as the anodic current pulse is applied. Examination of the dE/dt vs. t plot shown in Figure 5(b) reveals that $Mn(OH)_2$ is oxidized in more than two steps during the anodic current pulse. These reaction steps might be oxidation to MnOOH at the potential corresponding to A2 and further oxidation of $Mn(OH)_2$ to MnO_2 and/or other oxide/hydroxide layer such as $MnO_x(OH)_y$ in the potential region of A1. The gradual potential change observed in the potential region of A1 suggests that more than one process is convoluted under a single CV peak. The potential changes sharply at A2 in contrast to that at A1; this is clearly shown

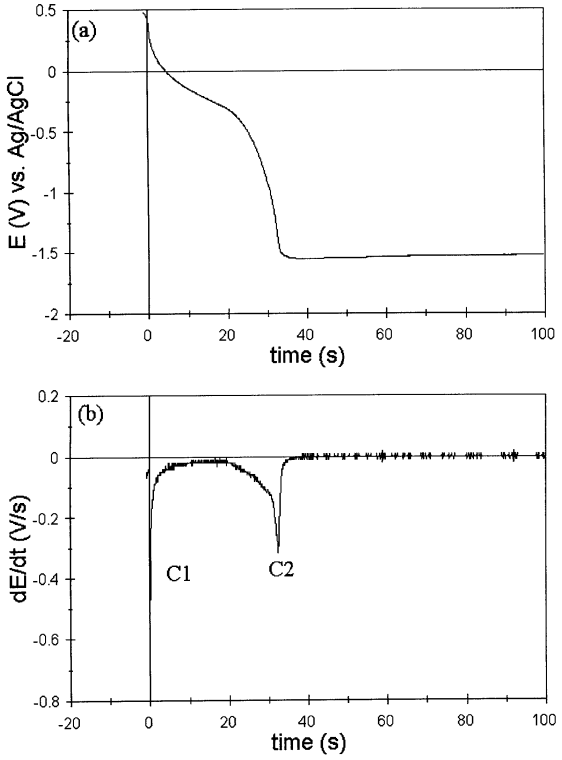

FIGURE 6. (a) CHRONOPOTENTIOGRAM RECORDED FOR CATHODIC REDUCTION IMMEDIATELY FOLLOWING CORRESPONDING ANODIC OXIDATION SHOWN IN FIGURE 5. THE APPLIED CURRENT WAS 0.15 mA. (b) CORRESPONDING dE/dt VS. t PLOT.

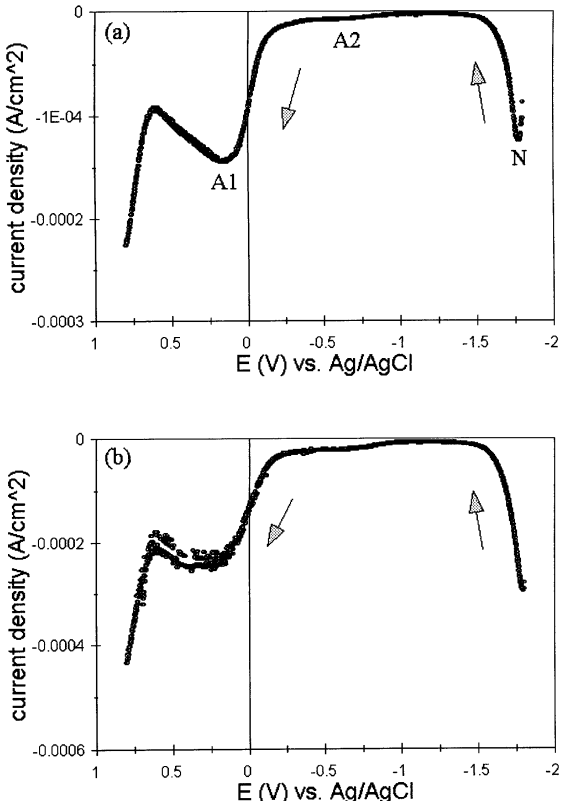

FIGURE 7. (a) DIFFERENTIAL PULSE VOLTAMMOGRAM RECORDED FOR OXIDATION OF MANGANESE ELECTRODE IN 0.10 *M* KOH; SCAN RATE = 20 mV/s, PULSE HEIGHT = 25 mV, PULSE WIDTH = 50 ms. (b) SAME AS IN FIGURE 7(a) EXCEPT SCAN RATE = 36 mVs AND PULSE HEIGHT = 50 mV.

by a current reversal chronopotentiogram described below.

A current reversal chronopotentiogram recorded during a cathodic current step of 0.15 mA is shown in Figure 6(a), which shows that $Mn(OH)_2$ is regenerated upon current reversal. Major changes in potentials are indicated more clearly in the dE/dt vs. t plot shown in Figure 6(b). The results shown here indicate that $Mn(OH)_2$ must be produced by the reduction of higher valence oxides in two steps. The processes taking place at C1 and C2 must correspond to the reversal processes of A1 and A2, respectively. Note that the redox processes in the regions of A2 and C2 are more rapid than those in the regions of A1 and C1. While this transition was not seen clearly in cyclic voltammograms, it is in chronopotentiograms.

Differential pulse voltammetry

Figure 7 shows typical differential pulse voltammograms recorded at the manganese electrode. A sharp peak, N, at -1.77 V and a large peak, A1, at about +0.17 V shown in Figure 7(a) are in excellent accord with the regions marked in Figure 1. A very broad, small peak, A2 shown in Figure 7(a), corresponds to the oxidation of C2 shown in

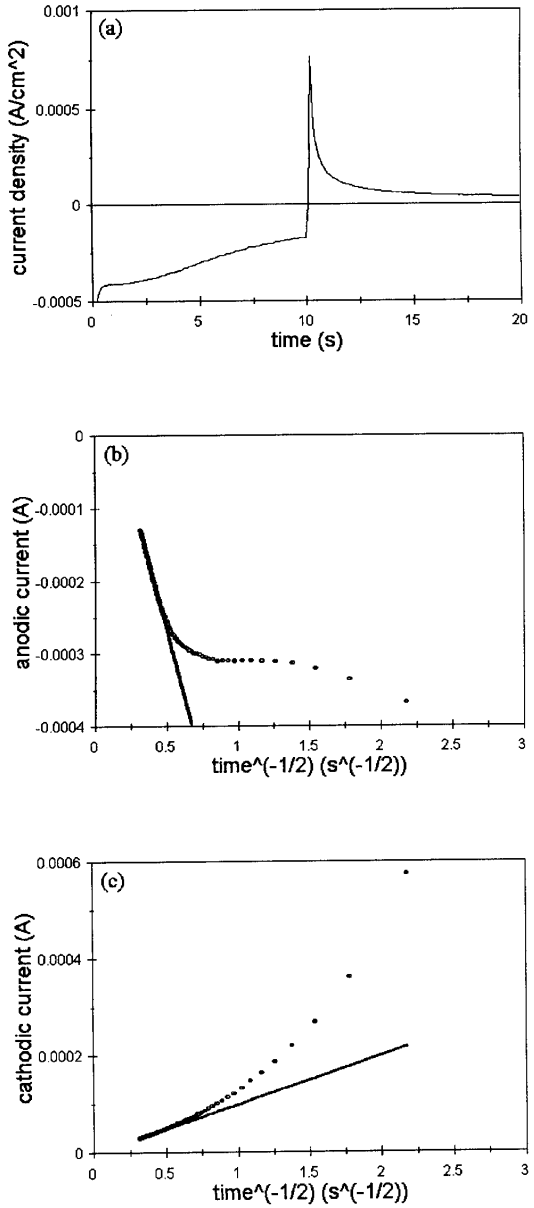

FIGURE 8. (a) CHRONOAMPEROMETRIC CURVE RECORDED AFTER FORWARD POTENTIAL STEP TO +0.20 V AND REVERSAL POTENTIAL STEP TO -1.50 V; (b) I(t) VS. $t^{-1/2}$ PLOT FROM DATA IN FIGURE 8(a) FOR ANODIC PROCESS; AND (c) I(t) VS. $t^{-1/2}$ PLOT FROM DATA IN FIGURE 8(a) FOR CATHODIC PROCESS.

Figure 1. Figure 7(b) displays the results obtained when the pulse height is increased to twice that used in Figure 7(a). The A1 peak becomes more noisy while the A2 peak becomes a little larger. A sharp peak, N, at -1.77 V (vs. Ag/AgCl in saturated KCl) is assigned to the oxidation of manganese to $Mn(OH)_2$ according to the reaction,

$$Mn + 2OH^- = Mn(OH)_2 + 2e^-. \quad (5)$$

This potential is in excellent agreement with the one in the literature, -1.56 V vs. SHE [27]. The broad peak, A2, at about -0.69 V must be the oxidation of Mn(II) to Mn(III) according to the reaction,

$$Mn(OH)_2 + OH^- = MnOOH + H_2O + e^-. \quad (6)$$

This potential is in good agreement with that published in the literature, -0.57 V vs. Ag/AgCl [23].

Chronoamperometry

Since the electrochemical behavior shown here can be described by a semi-infinite model as concluded from the scan rate dependency of the CV peak currents, we examined the reaction by using another transient technique, chronoamperometry. A double potential step chronoamperometric (CA) curve recorded after the potential (not shown) was stepped to -0.65 V followed the simple Cottrell equation,

$$i(t) = nFAD^{1/2}C^*/(\pi^{1/2}t^{1/2}), \quad (7)$$

which confirms that the electrochemical process is diffusion controlled. A double potential step CA curve recorded when the potential was stepped to +0.20 V is not as straightforward as shown in Figure 8. The anodic decay curve is much more complex than that of the cathodic decay. During the anodic process, there appear at least two time domains, in which more than one electrochemical reaction must take place. These electron transfer steps may include oxidation of $Mn(OH)_2$ to MnOOH taking

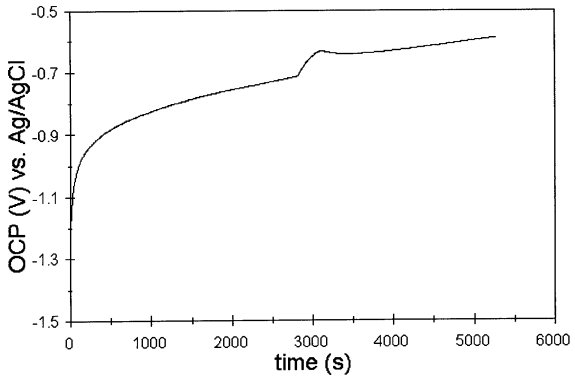

FIGURE 9. OPEN CIRCUIT POTENTIAL PROFILE MEASURED FOR A FRESHLY PREPARED FILM OF $Mn(OH)_2$ AT THE MANGANESE ELECTRODE IN 0.10 *M* KOH SOLUTION.

place between about 0.2 and 1.5 s and oxidation of $Mn(OH)_2$ to higher valence oxides/hydroxides outside this time domain. These changes are shown more clearly in the i(t) vs. $t^{-1/2}$ plot (Figure 8[b]).

These experiments illustrate the complexity of the oxidation of $Mn(OH)_2$ to higher valence oxides. They also support results obtained from chronopotentiometry and differential pulse voltammetry experiments, where the oxidation of $Mn(OH)_2$ to MnOOH has been clearly identified.

Open circuit potential measurement

Figure 9 shows the result of open circuit potential (OCP) measurements in the same electrolyte solution, and the result is also revealing. After the circuit was open with the electrode polished and reduced cathodically at -1.50 V for 2 hours to first remove the oxide films, the OCP increased quickly to about -1.04 V in less than a minute, which was followed by a slow increase to -0.71 V in 47 min. The rapid increase in potential may result from the oxidation of manganese perhaps by water according to the reaction,

$$2Mn + 4H_2O \rightarrow 2Mn(OH)_2 + 2H_2, \quad (8)$$

underneath the already present $Mn(OH)_2$ film. The slow increase to -0.71 V may arise from the further oxidation of $Mn(OH)_2$ to MnOOH by a trace amount of oxygen in water,

$$4Mn(OH)_2 + O_2 \rightarrow 4MnOOH + 2H_2O, \quad (9)$$

which is expected to proceed slowly due to the limited amount of oxygen. This range of the OCP corresponds to the peak A2 shown in Figure 7. It is interesting to note that the OCP increases rapidly during the oxidation to $Mn(OH)_2$ until about 52 min, when it decreases again. The slight decrease in the OCP could have resulted from the disproportionation reaction of thus produced MnOOH [9].

CONCLUSIONS

In the first step of oxidation, the manganese metal is oxidized to initially form manganese(II) hydroxide, which is known to passivate the metal surface. The redox process between $Mn(OH)_2$ and Mn is chemically reversible. The $Mn(OH)_2$/Mn system in alkaline media has the hydrogen evolution process as the major competing reaction. The manganese(II) hydroxide undergoes further oxidation to manganese(III) oxyhydroxide and/or manganese oxides/hydroxides of higher valences depending on the potential region. The Mn(II)/Mn(0) and Mn(III)/Mn(II) pairs have been clearly identified in our experiments employing transient techniques other than voltammetry. These passivation layers of higher valences are believed to have mixed stoichiometries rather than a definite oxidation state [16].

The semi-infinite diffusion model has been demonstrated to be operative during the experimental time domain. The fact that the

semi-infinite diffusion model is at work during the manganese oxidation indicates that the $Mn(OH)_2$ film, not manganese, is oxidized to manganese oxides/hydroxides of higher valences. The manganese metal at the metal-oxide interface could be oxidized to Mn(II) hydroxide near the transpassivation region by perhaps its own oxide,

$$Mn + MnO_2 + 2H_2O \rightarrow 2Mn(OH)_2. \quad (10)$$

Thus the $Mn(OH)_2$ film becomes thicker as the number of potential cycles increases. This film behaves as an electroactive film for further oxidation.

It is concluded that the electrochemical oxidation of $Mn(OH)_2$ at manganese electrode can be described as a diffusion-controlled process. The redox process is limited by the transport of reactant species through the film formed on the electrode surface. The CA experiments provide an insight into a series of the film formation processes taking place upon oxidizing $Mn(OH)_2$. The electron transfer kinetics depend on the surface films formed during the electrochemical reaction. It is concluded that the redox currents are affected strongly by the presence of the film due to the difference in electron transfer rates at different potentials (Figure 8). The exchange rate constant is 6.2×10^{-8} cm/s for the oxidation of $Mn(OH)_2$ to higher oxidation states.

ACKNOWLEDGMENT

The U.S. Department of Energy, Office of Restoration and Waste Management, Office of Technology Development, provided support for this research through the Waste-Management Education and Research Consortium (WERC).

REFERENCES

1. A. Kozawa and J.F. Yeager, J. Electrochem. Soc., 112 (1965) 959.

2. A. Kozawa and RA. Powers, J. Electrochem. Soc., 113 (1966) 870.

3. A. Kozawa and J.F. Yeager, J. Electrochem. Soc., 115 (1968) 1003.

4. A. Kozawa, In: K.V. Kordesch (Ed.), Batteries, Marcel Dekker, New York 1974.

5. M. Fleischmann, H.R. Thirsk, and I.M. Tordesillas, Trans. Faraday Soc., 58 (1962) 1865.

6. R.L. Paul and A. Cartwright, J. Electroanal. Chem., 201 (1986) 113.

7. R.L. Paul and A. Cartwright, J. Electroanal. Chem., 201 (1986) 123.

8. D. Gosztola and M.J. Weaver, J. Electroanal. Chem., 271 (1989) 141.

9. W.-H. Kao and V.J. Weibel, J. Appl. Electrochem., 22 (1992) 21.

10. D.Y. Qu, B.E. Conway, L. Bai, Y.H. Zhou, and W.A. Adams, J. Appl. Electrochem., 23 (1993) 693.

11. L. Bai, D.Y. Qu, B.E. Conway, Y.H. Zhou, G. Chowdhury, and W.A. Adams, J. Electrochem. Soc., 140 (1993) 884.

12. B.D. Desai, J.B. Fernandes, and V.N. Kamat Dalal, J. Power Sources, 16 (1985) 1.

13. A.T. Kuhn and T.H. Randle, J. Chem. Soc., Faraday Trans., 79 (1983) 417.

14. T.H. Randle and A.T. Kuhn, Aust. J. Chem., 42 (1989) 1527.

15. H. Zhang and S.-M. Park, J. Electrochem. Soc., 141 (1994) 2422.

16. J. Brenet, J.P. Gabano, and J. Reynaud, Electrochim. Acta, 8 (1963) 207.

17. L.D. Burke and O.J. Murphy, J. Electroanal. Chem., 109 (1980) 373.

18. F. Chouaib, P. Heubel, M. Sanson, G. Picard, and B. Tremillon, J. Electroanal. Chem., 127 (1981) 179.

19. M. Gonsalves and D. Pletcher, J. Electroanal. Chem., 285 (1990) 185.

20. J. Ambrose and G.W.D. Briggs, Electrochim. Acta, 16 (1971) 111.

21. G.W.D. Briggs and D.F. Davies, Electrochim. Acta, 24 (1979) 439.

22. S.I. Cordoba, R.E. Carbonio, M.L. Teijelo, and V.A. Macagno, Electrochim. Acta, 31 (1986) 1321.

23. M.H. Ubeda, H.T. Mishima, and B.A.L. Mishima, Electrochim. Acta, 36 (1991) 1013.

24. D.D. McDonald, Corros. Sci., 16 (1976) 461.

25. T.A. Zordan and L.G. Hepler, Chem. Rev., 68 (1968) 737.

26. O. Bricker, Am. Miner., 50 (1965) 1296.

27. A.J. Bard, R. Parsons, and J. Jordan, Standard Potentials in Aqueous Solutions, Marcel Dekker Inc., New York, 1985.

28. C-H. Pyun and S.-M. Park, J. Electrochem. Soc., 133 (1986) 2024.

29. C. Zhang and S.-M. Park, J. Electrochem. Soc., 134 (1987) 2966.

30. C. Zhang and S.-M. Park, J. Electrochem. Soc., 136 (1989) 3333.

31. H. Zhang and S.-M. Park, J. Electrochem. Soc., 141 (1994) 718.

32. (a) H. Zhang and S.-M. Park, J. Electrochem. Soc., 141 (1994) 2001; (b) also, Electrochemically deposited thin films, In: M. Paunovic, I. Ohno, and Y. Miyoshi (Eds.), Electrochemical Society Proceedings, Vol. 93-21, Pennington, NJ, 1993.

33. B.-S. Kim, T. Piao, S.N. Hoier, and S.-M Park, Corrosion Sci., 37 (1995) 557.

34. M. Cai and S.-M. Park, J. Electrochem. Soc., (1996) in press.

35. H. Zhang and S.-M. Park, Carbohydrate Research, 266 (1995) 129.

36. M. Pourbaix, Atlas of Electrochemical Equilibria in Aqueous Solutions, Pergamon Press, Ltd., London, 1966.

37. H.A. Dessouki, A.A. Abdel Fattah, G.E. El Sayed, and S.M. Abd El Haleem, Corros. Prev. & Control, 37 (1990) 69.

38. R.S. Nicholson and I. Shain, Anal. Chem., 36 (1964) 706.

39. W.M. Latimer, Oxidation States of the Elements and their Potentials in Aqueous Solutions, 2nd ed., Prentice-Hall, New Jersey, 1952.

40. D.M. MacArthur, J. Electrochem. Soc., 117 (1970) 422.

41. J.E.B. Randles, Trans. Faraday Soc., 44 (1948) 327.

42. A. Sevcik, Collect. Czech. Chem. Commun., 13 (1948) 349.

43. P.E. Sturrock, J.L. Hughey, B. Vaudreuil, G. O'Brien, and R.H. Gibson, J. Electrochem. Soc., 122 (1975) 1195.

44. P.E. Sturrock and R.H. Gibson, J. Electrochem. Soc., 123 (1976) 629.